CrossMark

Flow field analysis of a passive wavy micromixer with CSAR and ESAR elements

Ranjitsinha R. Gidde[1] · Prashant M. Pawar[1] · Babruvahan P. Ronge[1] · Anil B. Shinde[1] · Nitin D. Misal[1] · Sandeep S. Wangikar[1]

Abstract

The performance analysis of wavy micromixers with split and recombine (SAR) elements has been carried out. The two types of SAR elements viz. circular split and recombine elements and elliptical split and recombine elements are used to get benefit of SAR mechanism. The main concept in the proposed design is to enhance the interfacial area between the two fluids by creating a transverse flow and split and recombination of fluid flow streams with the help of SAR elements. The effects of balanced split and unbalanced split of SAR elements and operational parameter Reynolds number on the mixing index and pressure drop are evaluated. The COMSOL Multiphysics 5.0 is used for computational fluid dynamics analysis of micromixers. The analysis is carried out for balanced and unbalanced split of the mixing elements at various Reynolds numbers in the range of 0.1–75. The computation interfacial patterns on the planes perpendicular to the direction of fluid flow, mixing index and pressure drop are studied in depth. The results indicate that at inlet Reynolds number below 5, the mixing performance is diffusion dominated. However at Reynolds number greater than 5, the mixing index increases intensely due secondary flow and separation vortices, as well as SAR effect.

1 Introduction

One of the essential process for Lab-On-a-Chip (LOC) devices is microscale mixing. In current scenario, micromixer has been broadly employed in biological analysis and chemical synthesis as an important component in LOC and micro-total analysis systems (μTAS) (Nguyen and Wu 2004; Hardt et al. 2005). In general, micromixers are classified into two types: active and passive. An active micromixer needs an external source of energy whereas a passive micromixer does not require any external source of energy. Hence, the structures of active micromixers are often complicated (Tran-Minh et al. 2014). In contrast to active micromixer, a passive micromixer are more attractive due to their features such as simple fabrication, absence of moving components.

Several studies engaged T-mixers to generate chaotic and turbulent flows for the rapid mixing (Wong et al. 2003). The mixing process in the 3D T-shaped and double T-shaped micromixers has been studied numerically to increase the mixing region (Izadpanah et al. 2018). The micromixers with different chambers and obstacles studied to obtain an optimum design configuration of the micromixer. In order to evaluate the overall performance of the micromixers, the ratio of the mixing index to the pressure drop (MI/PD) was selected as a criterion (Cheri et al. 2013). A 3D serpentine microchannel is designed to generate rapid stretching and folding of the fluid streams, to promote chaotic advection. However, a relatively high Reynolds number (> 25) was required to generate the chaotic advection (Liu et al. 2000). A 3D twisting flow mechanism in a microchannel is achieved by providing diagonally oriented ridges on the bottom wall of the channel. A staggered herringbone structure patterns have been developed at the bottom of the microchannel, in which chaotic mixing is obtained by alternating velocity fields (Stroock et al. 2002). A micromixer with curved microchannels based on split and recombine mixing mechanism was investigated. The micromixer was designed to keep the main channel as well as the sub-channels in curved shape to induce Dean vortices (Mouza et al. 2008). A P-SAR micromixer with fan-shaped cavities has been studied. The enhancement in mixing performance

✉ Ranjitsinha R. Gidde
  ranjitsinhag1@rediffmail.com

[1] SVERI's College of Engineering, Pandharpur, Maharashtra 413304, India

achieved by a synergistic effect due to unbalanced inertial collision between the streams, Dean and expansion vortices (Xia et al. 2012). Furthermore, the modified P-SAR micromixer with dislocation sub-channels has been established using similar principles wherein rapid and efficient mixing achieved for the wide range of Reynolds numbers (Li et al. 2013). Taguchi method has been employed to optimize planar micromixer with mixing units combining gaps and baffles (Shih and Chung 2008). The novel parallel laminar micromixer with two-dimensional staggered curved channels with tapered structures has been demonstrated wherein Dean vortex flows produced in curved rectangular channels by means of centrifugal forces (Sheu et al. 2012). A serpentine microchannel with semicircular obstacles and straight and serpentine micro-channels have been studied numerically and experimentally (Wangikar et al. 2017; Das et al. 2017).

Numerous fabrication techniques have been reported by many researchers to fabricate micro-channel on glass substrate. These include wet chemical etching, micro-contact printing and wet chemical etching, dry etching process such as deep reactive ion etching (DRIE). Wire-cut electro discharge machining (WEDM) and ultrasonic machining (USM) have been used as manufacturing processes for manufacturing the serpentine with square, circular, and zigzag profile micro-channels (Das and Patowari 2018). The PDMS replica molding method has used to fabricate rectangular wave micromixer (RWM), which includes steel based mold fabricated using WEDM. These master molds have been employed for making poly-dimethylsiloxane (PDMS) based micromixer using soft lithography (Gidde et al. 2018). A novel micromixer with gaps and baffles is manufactured from PDMS based on the soft lithography technique in the clean room (Xia et al. 2016). The PDMS replica molding method has used to fabricate the passive micromixer based on unbalanced splits, which involves preparing the SU-8 resist mold over a silicon wafer by photolithography and transferring the pattern of the micromixer to PDMS replica (Ansari et al. 2010).

As discussed above, a variety of experimental and numerical studies have been carried out for different types of passive micromixers. However, no one has carried out investigation regarding wavy micromixer with SAR mixing segments placed at equidistant along the stream trajectory length of the micromixer. The present study conducts a computational fluid dynamic investigation of mixing performance for a novel wavy micromixer with SAR mixing segments, which uses lamination, chaotic and SAR mechanisms comprehensively. The fluid flow and mixing process are investigated by numerical simulations. In the present paper, the effect of balanced split and unbalanced split of the fluid streams on the mixing performance is analyzed. Moreover, the influence of ratio of width of splits on the comprehensive performance of micromixers is studied based on different evaluation performance criteria.

2 Physical model and numerical formulation

Figure 1 shows schematic models of the wavy micromixer with CSAR and ESAR elements based on the concept of SAR mechanism and cross-collisions of fluid streams. The two fluids separately enter through two inlets and come into contact at a T-junction where they undergo some mixing before entering the micromixer and thence to wavy channel and CSAR and ESAR elements along the stream wise length of channel. The channel is split into two sub-channels of equal widths and unequal width for both type of micromixers.

The flows in microchannels are laminar flows. Hence, it is very difficult to achieve turbulent mixing in a microchannel. For enhancing mixing, it is possible to induce flow separation and secondary flows by providing sharp turns, junctions, obstacles, and discontinuities in the path of the flow (Alam and Kim 2012). When the fluid streams pass through a sharp turn, a secondary flow perpendicular to the flow path occurs. Further, the formation of vortices is occurred due to separation of the boundary layer. Vortices can be created by the twisting and breaking of stream layers which results in better mixing performance. Vortex formation is depending on the geometry of the microchannel and the Reynolds number. Any agitation
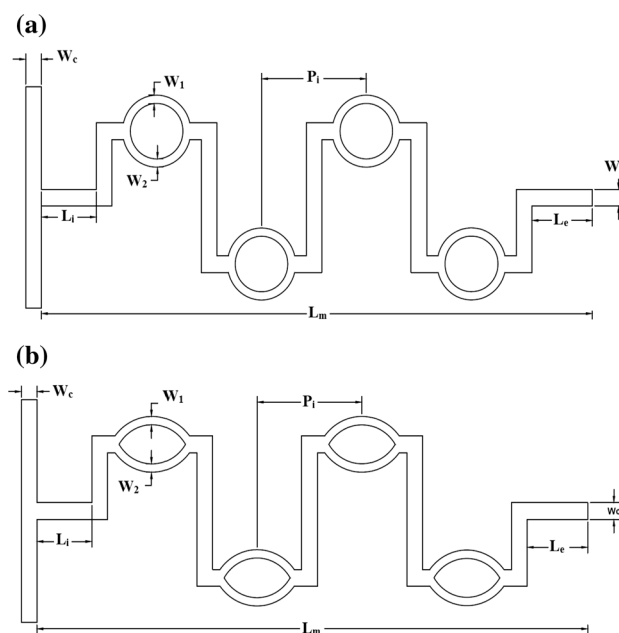
Fig. 1 Schematic illustrations of micromixers with **a** CSAR elements and **b** ESAR elements

of the flow creates a lateral movement that stretches the interface between the fluids and increases the rate of mixing. The chaotic advection mechanism can be easily generated by special channel geometries that split, stretch, fold and break the flow (Lin 2015).

In the present work, a wavy micromixers with circular SAR and elliptical SAR elements along the stream trajectory length are designed. Each micromixer design consists of four SAR elements. The dimensions of the microchannel are as follows: width of the channel, W_c = 0.3 mm, height of the channel, H_c = 0.3 mm, and length of the inlet channel, L_i = 1.05 mm, length of the exit channel, L_e = 1.15 mm, pitch between the two SAR elements, Pi = 2 mm and axial length of channel, L_m = 10.5 mm.

2.1 Governing equations

2.1.1 Flow computation

The flow and mixing behavior is analyzed using the CFD software COMSOL Multiphysics 5.0. Fluid flow inside the microchannel is governed by the incompressible Navier–Stokes equations which include the continuity and momentum Eqs. (1) and (2), respectively (Gidde et al. 2018).

$$\nabla u = 0, \tag{1}$$

$$\rho \left[\frac{\partial u}{\partial t} + (u.\nabla)u \right] = -\nabla p + \mu \nabla^2 \mathrm{u}. \tag{2}$$

2.1.2 Species transport

The convection–diffusion equation which governs the mass transport in the case of the steady state in the three-dimensional microchannel is written as Eq. (3) (The et al. 2015):

$$\frac{\partial c}{\partial t} = D\nabla^2 c - u.\nabla c, \tag{3}$$

where u is the fluid velocity, p is the fluid pressure, ρ is the fluid density, μ is the fluid viscosity, D is the diffusivity, and c is the molar concentration.

2.2 Boundary conditions

The pure water and ethanol fluids flow into the micromixer through inlet 1 and inlet 2 respectively. The main reason for choosing water and ethanol is that there are some studies on mixing with these fluids. The second reason is that the physical properties, especially diffusivity of both fluids are quite suitable for numerical analysis (Ansari et al. 2010). The physical properties of water and ethanol at

20 °C are given in Table 1. At the two inlets, constant concentrations of 0 and 1 (mol/m^3) are applied. Zero static pressure is specified at the flow outlet. At all the channel walls no-slip boundary conditions are used. The influence of the gravity force is not considered, and it is assumed that chemical reaction does not occur. All the simulations are performed at the constant temperature of 20 °C.

For numerical simulation, an inlet flow rates at the cross-section area of channel inlet corresponding to Reynolds number in the range from 0.1 to 75 are calculated and employed in simulations. The Reynolds number is defined as follows:

$$Re = \frac{\rho U D_h}{\mu}, \tag{4}$$

where, ρ is the average density of fluids, U is the average velocity of the fluids in the inlet channel, D_h is the hydraulic diameter of the inlet channel and μ is the average absolute viscosity of the fluids. It is essential to consider another characteristic dimensionless number Peclet number, in order to investigate the mixing index of the micromixer. Peclet number is defined as given below by Eq. (5):

$$Pe = \frac{U D_h}{D}. \tag{5}$$

3 Micromixer evaluation characteristics

For the evaluation of the overall performance of the micromixers the following characteristics viz., mixing index and pressure drop are used.

3.1 Mixing index

The mixing index and pressure drop are used to analyze the efficiency of the micromixers for different design requirements. The mixing index is required to represent homogeneity, mixing quality of mixed fluid in micromixers. It also reflects the uniform degree of species concentration in the micromixer. The output of CFD can be employed to determine the degree of mixing quality or mixing index.

Table 1 Properties of two working fluids at 20 °C

Properties	Water	Ethanol
D (m^2/s)	1.2×10^{-9}	1.2×10^{-9}
ρ (kg/m^3)	998	789
μ (Pa.s)	0.9×10^{-3}	1.2×10^{-3}
C (mol/m^3)	0	1

The expressions used to determine mixing index are as follows (Gidde et al. 2017):

$$\sigma^2 = \frac{1}{N} \sum_{i=1}^{N} (C_i - C_m)^2, \tag{6}$$

$$MI = 1 - \sqrt{\frac{\sigma^2}{\sigma_{max}^2}}, \tag{7}$$

where N represents the number of sampling points on the cross-section plane under consideration, C_i and C_m represent the mass fraction of sampling point i and the optimal mass fraction, respectively. σ denotes the standard deviation of concentration and σ_{max} is the maximum standard deviation of concentration in the specific cross-section perpendicular to the flow direction. MI ($0 \leq$ M.I. ≤ 1) is the mixing index in the specific cross-section. M.I. = 0 corresponds to no mixing (for which $\sigma = \sigma_{max}$) and M.I. = 1 a complete mixing (for which $\sigma = 0$).

3.2 Pressure drop

Apart from mixing index, the pressure drop along the stream trajectory length of the channel is another major parameter in the LOC application, which corresponds to pumping power. The pressure drop (ΔP) in the mixing channel is evaluated by the difference between the area-weighted average of total pressure on the outlet plane (P_o) and on a cross-section plane at the inlet (P_i) of the mixing channel (Cortes-Quiroz et al. 2014) and is expressed as given below:

$$\triangle P = P_i - P_o. \tag{8}$$

Moreover, for stationary microchannel, the flow is driven by an applied pressure gradient. The high pressure drop means that, the greater driving force and more power is needed. It is important to take pressure drop into account for micromixer design because high pressure drop is contrary to the chip encapsulation and integration (Xia et al. 2016). Hence, in evaluating the overall performance and reliability of the micromixer, the pressure drop must be considered together with mixing index. To study the mixing performance, simulations were performed at different flow rate, Reynolds number as listed in Table 2.

4 Results and discussion

4.1 Grid independency study

To perform numerical simulations, the preliminary grid independence test has been carried out with six different grid systems, for wavy micromixer with CSAR elements. The mixing index has been evaluated on the outlet plane across

Table 2 Flow inlet, Reynolds number and Peclet number value used in numerical simulation

Flow Inlet (ml/h)	Velocity (m/s)	Reynolds number	Peclet number
0.1088	0.0003	0.1	84
1.0879	0.0034	1	839
5.4393	0.0168	5	4197
10.8786	0.0336	10	8394
16.3179	0.0504	15	12591
21.7571	0.0672	20	16788
27.1964	0.0839	25	20985
32.6357	0.1007	30	25182
38.0750	0.1175	35	29379
43.5143	0.1343	40	33576
48.9536	0.1511	45	37773
54.3928	0.1679	50	41970
59.8321	0.1847	55	46167
65.2714	0.2015	60	50364
70.7107	0.2182	65	54561
76.1500	0.2350	70	58758
81.5893	0.2518	75	62955

the direction of flow along x-axis of wavy micromixer with CSAR elements for six grid systems in the range 68,515–327,210 as shown in Table 3.

The relative error can be calculated by using Eq. (9) (Xia et al. 2016):

$$e\% = \left| \frac{f_2 - f_1}{f_1} \right| \times 100. \tag{9}$$

According to the simulation results, the deviation of the mixing index for the grids between 243,054 and 327,210 is less than 0.01% (i.e. 0.0048). Consequently, a grid system with 243,054 elements has been adopted as the optimum grid system for further simulations. In addition the minimum element quality and average element quality are 0.4699 and 0.9470, respectively for the optimum grid system. The maximum element and minimum element sizes are 0.0225 and 0.0018 mm, respectively. The simulation result of velocity profile in x–y plane for the micromixer with CSAR elements corresponding to the

Table 3 Grid independency study

Grids	Mixing index	% Error
68515	0.89321	4.5730
82690	0.85415	2.9679
130042	0.82953	0.3666
172920	0.82650	0.0060
243054	0.82645	0.0048
327210	0.82641	0.0000
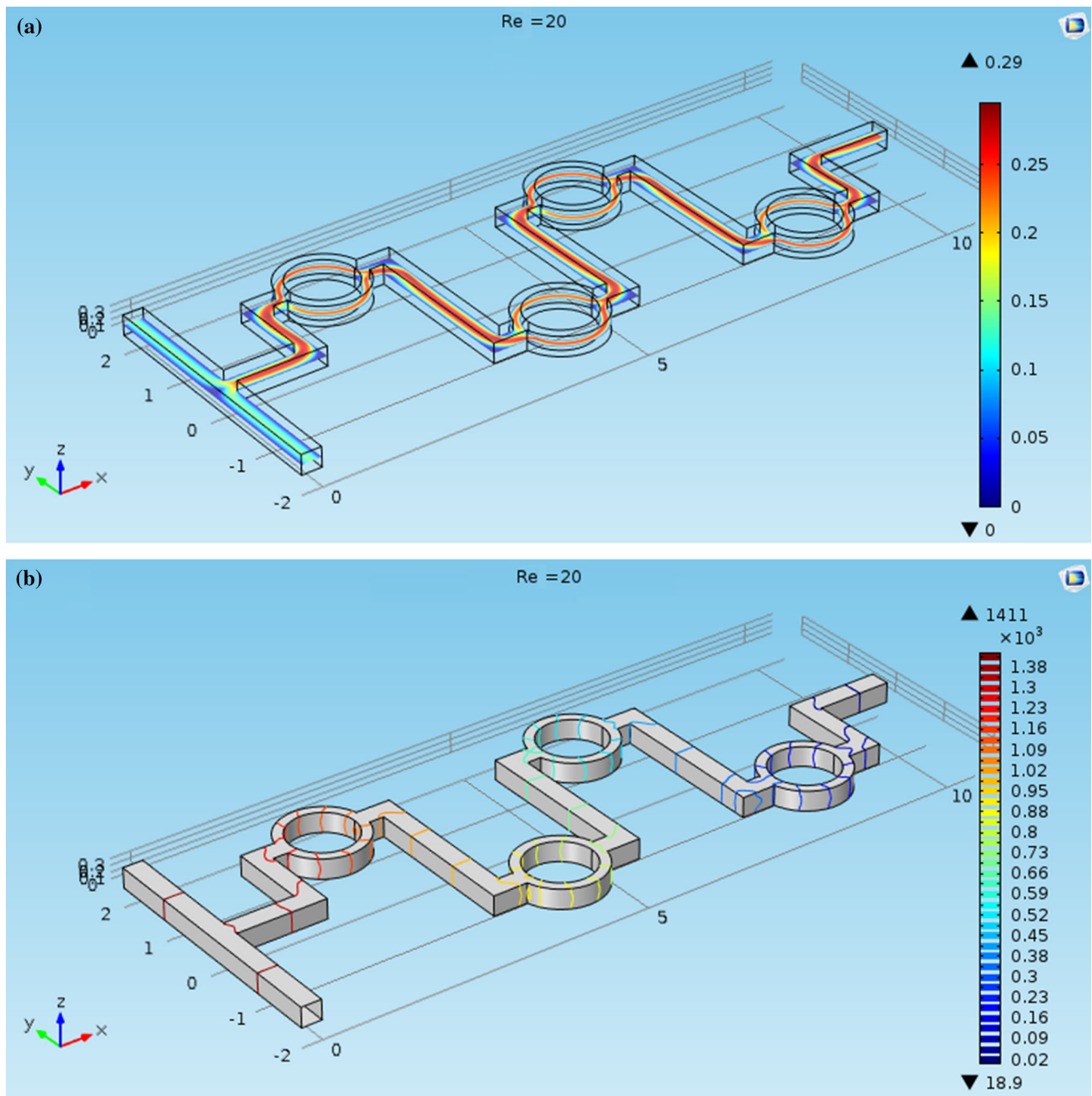
Fig. 2 Micromixer with CSAR elements with balanced splits. **a** Velocity magnitude in m/s at Re = 20, and **b** contour: pressure in Pa at Re = 20

Re = 20 is shown in Fig. 2a. It shows that the velocity is significantly higher at the place where the fluid stream is forced into circular SAR elements. Further, the simulation result for pressure drop at Re = 20 for micromixer with CSAR elements is shown in Fig. 2b.

4.2 Flow physics analysis

Study of internal dynamics of flow inside the micromixer is essential in designing micromixers adapted for specific requirements and applications. Thus, in the following sections, the general flow field analysis is discussed, and the fluid mixing mechanism is explained.

4.2.1 Micromixer with CSAR elements

The mixing performance for the micromixer with circular SAR elements is shown in Figs. 3, 4, and 5. Figure 3 shows the distributions of mass fraction on the x–y plane along the microchannel at Re = 20. During turning of the flow,
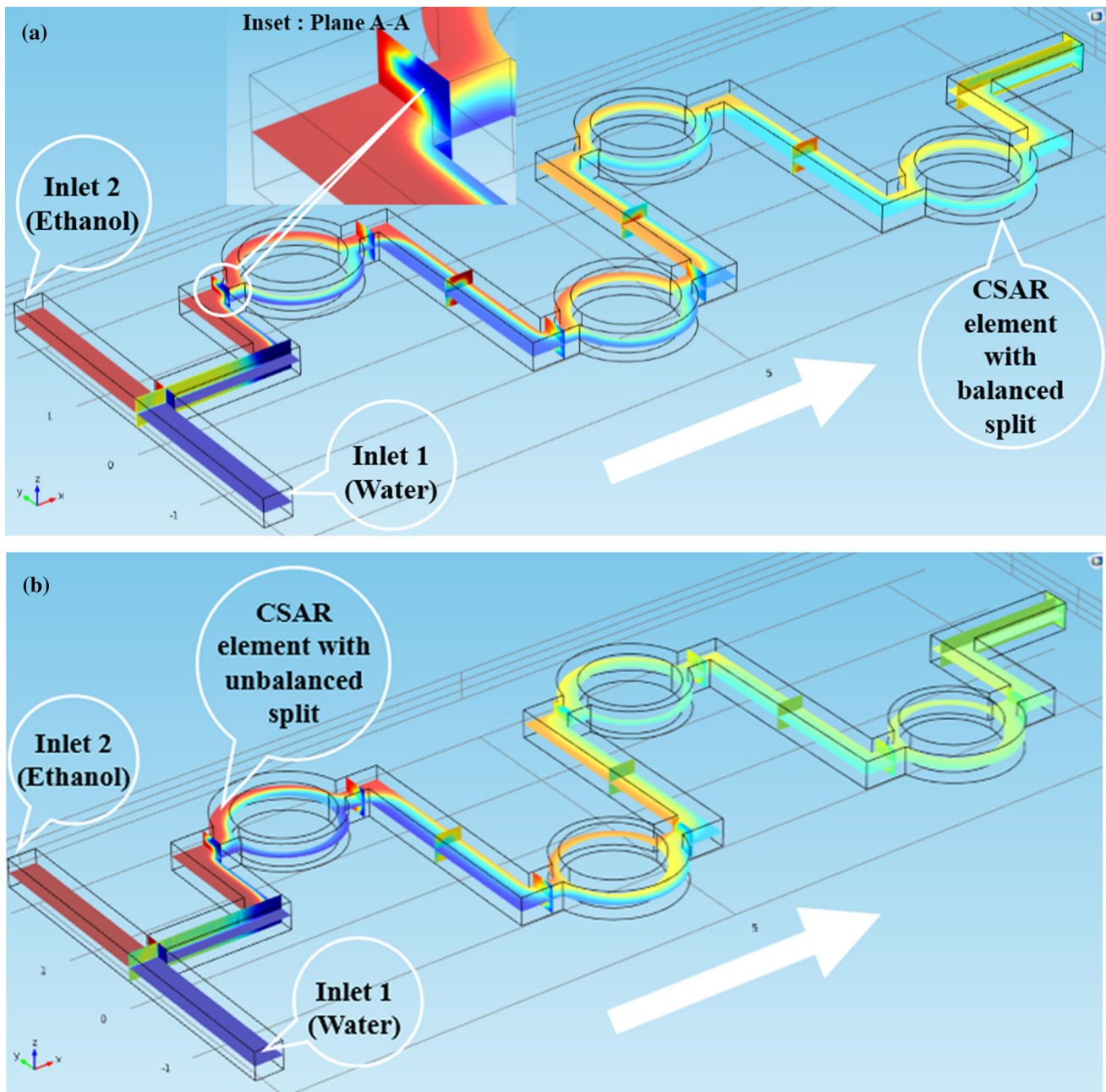
**Fig. 3** Distributions of mass fraction of ethanol on the x–y plane at the middle height of 150 μm and at various y–z planes along stream trajectory length of micromixer with CSAR elements with **a** balanced split and **b** unbalanced split at Re = 20

flow near the inner bend accelerates, and flow near the outer bend decelerates.

This resulted in the formation of vortices as shown in inset (Plane A–A) of Fig. 3a. The characteristics of the vortices depend upon degree of acceleration. Additionally enhancement in mixing takes place due SAR geometry of CSAR elements along the streamwise length of the micromixer. Figures 4 and 5 show the mass fraction of ethanol on the y–z plane and z-x planes at different positions for Re = 0.1, 5, 20, 45, 60, and 75 for CSAR with

balanced and unbalanced splits, respectively. The contours at different positions show the mixing behavior in the channel. For flow at low Reynolds number of Re = 0.1 (e.g., at the flow rate 0.1088 ml/h), the fluid interface distortion is minimal when the fluids pass each CSAR elements, and not much fluid stretching and folding can be observed in this case, as shown in Fig. 4. The details about various cross sectional planes and their distances from the confluence point are depicted in Table 4. The mixing process is predominantly due to molecular diffusion. A
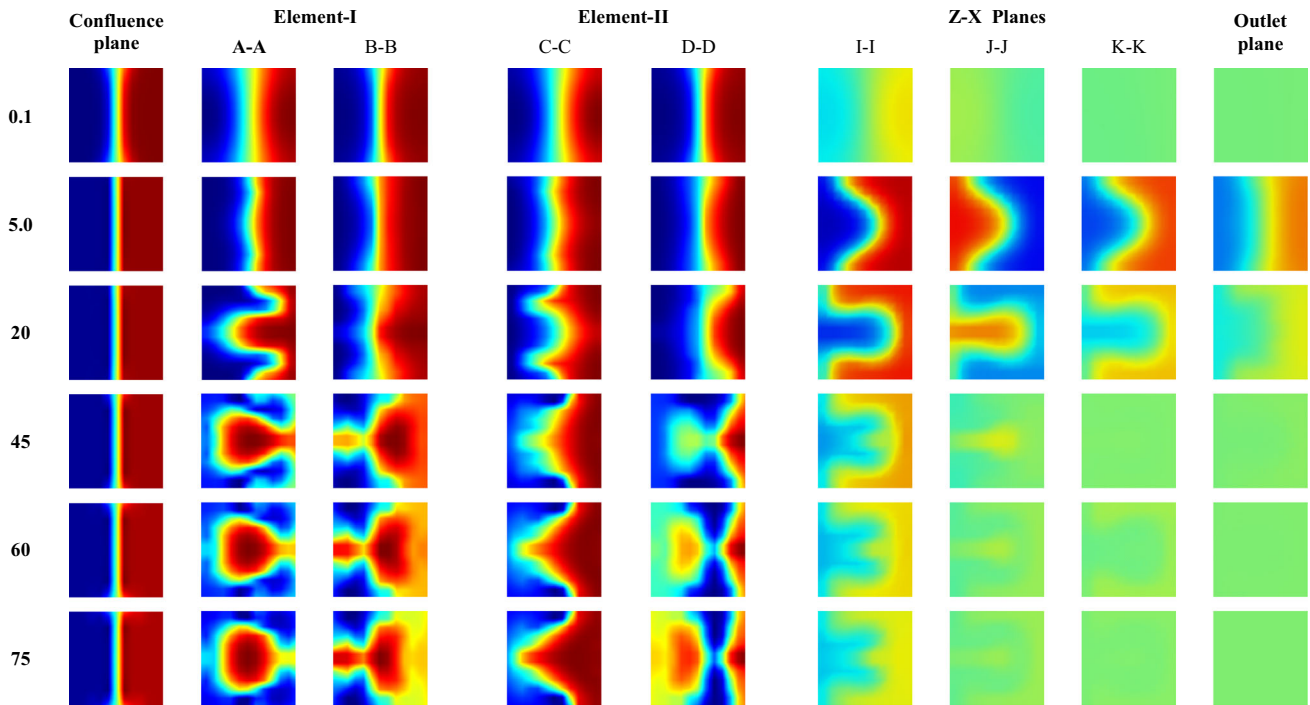
Fig. 4 Predicted concentration distributions at different planes for micromixer with CSAR elements with balanced split for Re = 0.1, 5, 20, 45, 60, and 75
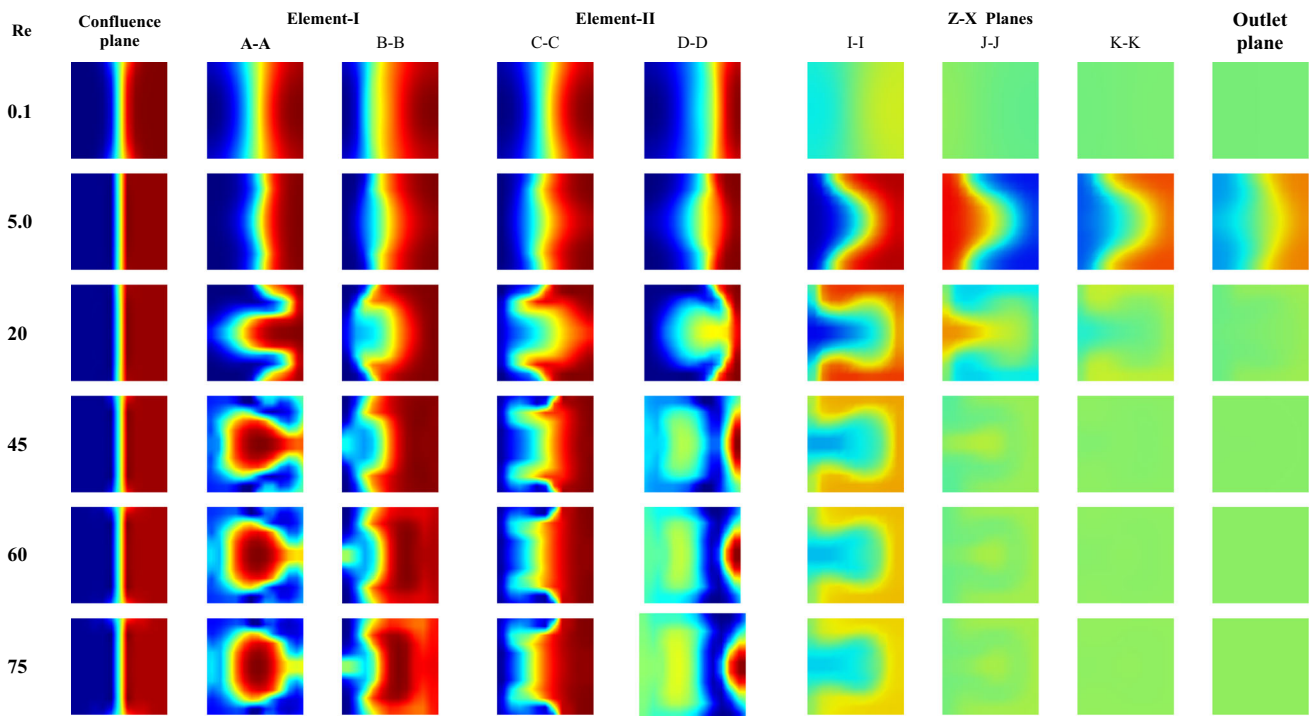
Fig. 5 Predicted concentration distributions of ethanol on different planes for micromixer with CSAR elements with unbalanced split for Re = 0.1, 5, 20, 45, 60, and 75

clear fluid interface can still be seen at the plane D–D, which indicates that the fluid mixing is still dominated by viscous forces. When the fluid velocity is increased to 5.4393 ml/h, with the inlet Reynolds number of 5, the fluid interface is slightly distorted as shown in Fig. 4. However, this distortion in the interface is not sufficient to achieve

Table 4 Cross sectional planes (y–z planes) and distance from the confluence point

Cross section plane	Distance from confluence (mm)	Remarks
A–A	1.4	Element-I
B–B	3.0	
C–C	3.4	Element-II
D–D	5.0	
E–E	5.4	Element-III
F–F	7.0	
G–G	7.4	Element-IV
H–H	9.0	
Outlet plane	10.5	Plane at the exit

enhanced mixing. At Re = 20 (flow rate, Q = 21.7571 ml/h), the transverse motion of the fluid can be seen, especially at the top and bottom portions of the channel close to the walls. This enhances mixing performance at the outlet plane. As the flow rate is continuously increased (> 21.7571 ml/h), the interfaces stretched and folded further, and transverse flow started to form.

In addition to this the fluid flows sequentially through the circular SAR elements, this transverse flow stirred the solutions rapidly, increased the interfacial area of the two fluids that reduce the diffusion distance in the transverse direction. Consequently, mixing in the micromixer is largely enhanced.

Also, the symmetry profile of mass fraction is observed at AA, BB, and CC planes for CSAR micromixer with balanced split and CSAR micromixer with unbalanced split, respectively at Re = 0.1. At Re > 5, the profiles become diverse due to the chaotic effect and SAR effect for both types of micromixers. As seen in Figs. 4 and 5, the profile of mass fraction ethanol develops with remarkable engulfment for both micromixers for Re = 20, 45, 60, and 75 at different y–z and z–x planes, respectively. By contrast, the significant variation of the interface shapes rather than the engulfment is observed in BB, CC, DD, and EE planes.

At the first element, the water surrounds the ethanol at AA plane for Re > 20, forming the round interface. The severe distortion occurs near both the top and bottom wall of channel. The mass flow rate in the major subchannel (subchannel with larger width), is greater than that in the minor sub-channel. Hence, the inertial effect to fluid in the major sub-channel is higher than that of the fluid in the minor subchannel.
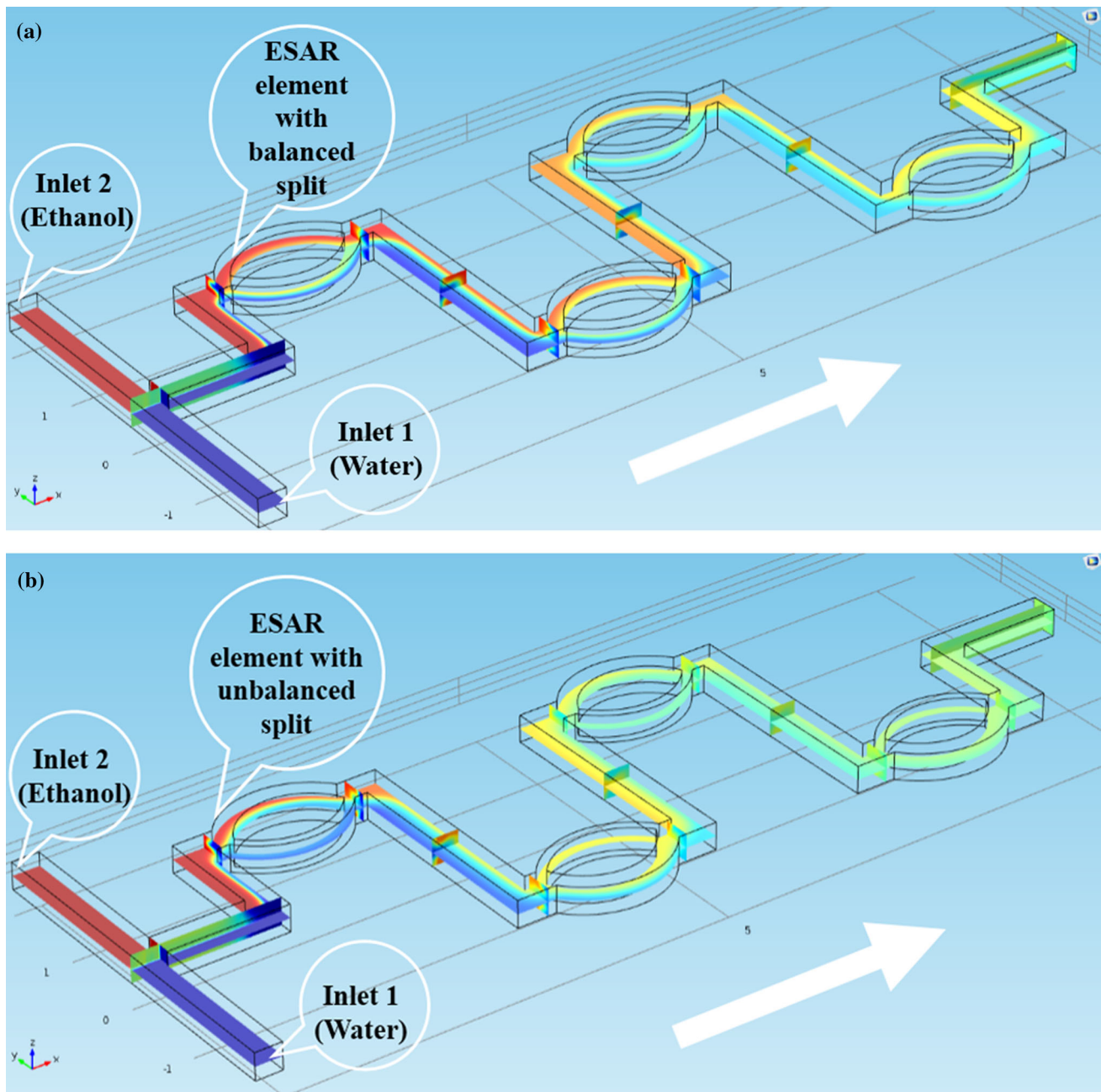
4.2.2 Micromixer with ESAR elements

The distributions of mass fraction of ethanol on the x–y plane and at various y–z planes along stream trajectory length for micromixer with ESAR elements at Re = 20 are shown in Fig. 6. The mechanism of mixing in the micromixer can be understood from the results of the flow field.

Figures 7 and 8 show the mass fraction of ethanol on the y–z plane and z–x planes at different positions for Re = 0.1, 5, 20, 45, 60, and 75 for ESAR with balanced and unbalanced splits, respectively. The mass fraction contours at different positions show the mixing behavior in the channel. The symmetry profile of mass fraction is formed at the confluence planes for both designs. At other planes, the profiles become diverse due to the individual chaotic effect of each micromixer and SAR mechanism. Thus the deformation of the interfacial lines is profoundly affected by secondary flow and related to the mixing characteristics.

At the confluence plane, the vertical interface is clearly visible and it starts distorting after the confluence plane by the combined effect of the secondary flow, separation vortices and SAR effect.

Furthermore, the interface between the two liquids is changed from straight to wave-shaped as observed in Fig. 7. In the case of wavy micromixers with balanced collisions mixing is poor due to the presence of only single fluid in sub-channels. The mixing is due to the chaotic advection and SAR mechanism without shifting of the interface of the fluid streams. In the case of unbalanced collisions of the fluid streams, the collisions perturb the flow and shift the interface of the fluid streams into the sub-channels where the engulfment takes place which in turn helps to enhance mixing. In addition, the mixing performance of micromixer with unbalanced split is efficient than the micromixer with balanced split. This enhancement in mixing performance is the result of a synergistic effect caused by unbalanced inertial collision between the streams. Accompanied by the SAR and the chaotic behavior, the concentration profile gradually becomes uniform. Among four micromixers, the micromixer with unbalanced splits exhibit the most uniform concentration profile at the y–z planes. The mass fraction of the ethanol on y–z planes, demonstrates the evident of good mixing at Re > 20. An excellent mixing quality in a micromixer is usually accompanied with a high pressure drop. The mass fraction of the ethanol on y–z planes, demonstrates the evident of good mixing at Re > 20. An excellent mixing

Fig. 6 Distributions of mass fraction of ethanol on the x–y plane at the middle height of 150 μm and at various y–z planes along stream trajectory length of micromixer with ESAR elements with **a** balanced split and **b** unbalanced split at Re = 20

quality in a micromixer is usually accompanied with a high pressure drop.

The flow physics analysis of both CSAR and ESAR reveals interesting behavior of the mixing index at Re = 5. The mixing in micromixers with CSAR and ESAR elements is dominated by molecular diffusion, which in turn due to the residence time and depends on the total path of the flow. At low Reynolds number i.e. at Re = 0.1 mixing index is higher due more residence time. When Re > 0.1, chaotic advection dominates the mixing performance with

the increase in Re. However, the chaotic advection at Re = 5 is not strong enough for better mixing. Hence a proper mixing has not been observed at Re = 5. Whereas, at Re > 5, the chaotic advection is increases with increase in Re. At higher Reynolds number i.e. beyond Re = 5, the mixing index is higher due to chaotic advection. Furthermore, Reynolds number of 5 can be considered as critical Reynolds number, indicating that transition in the mixing performance occurs comparatively at a low Reynolds number.
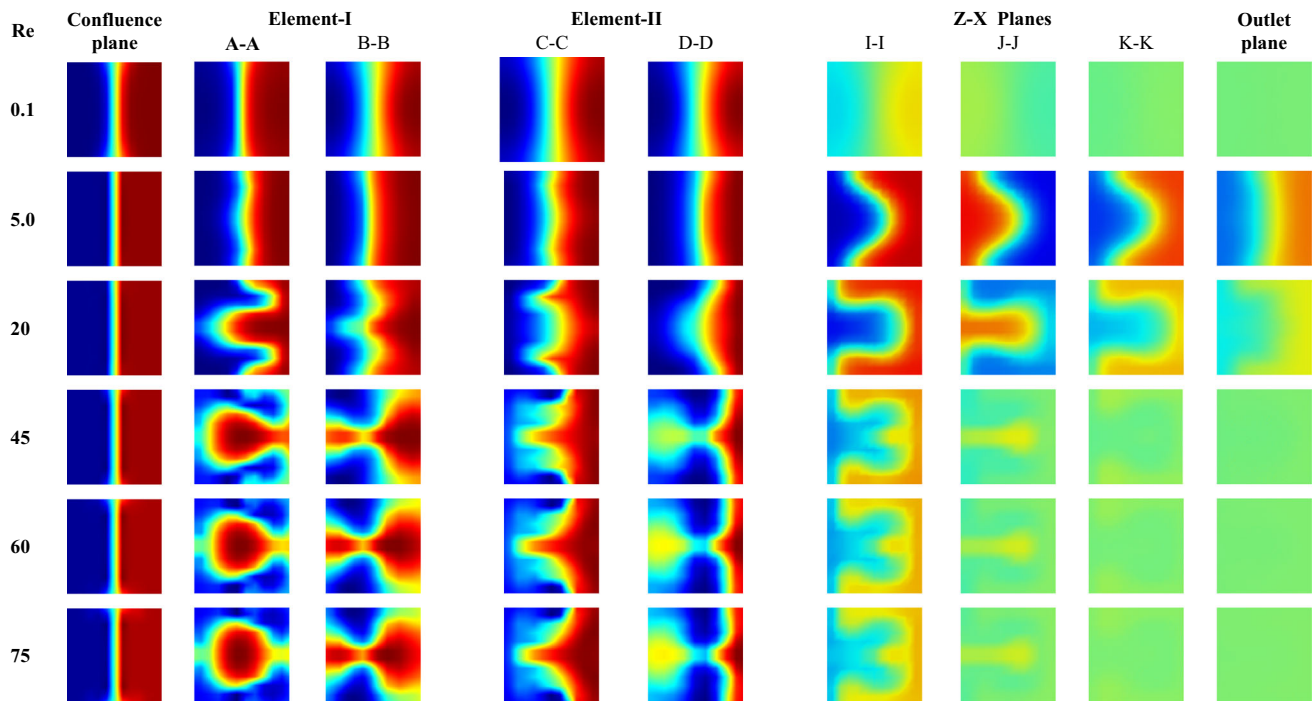
Fig. 7 Predicted concentration distributions at different planes for micromixer with ESAR elements with balanced split for Re = 0.1, 5, 20, 45, 60, and 7
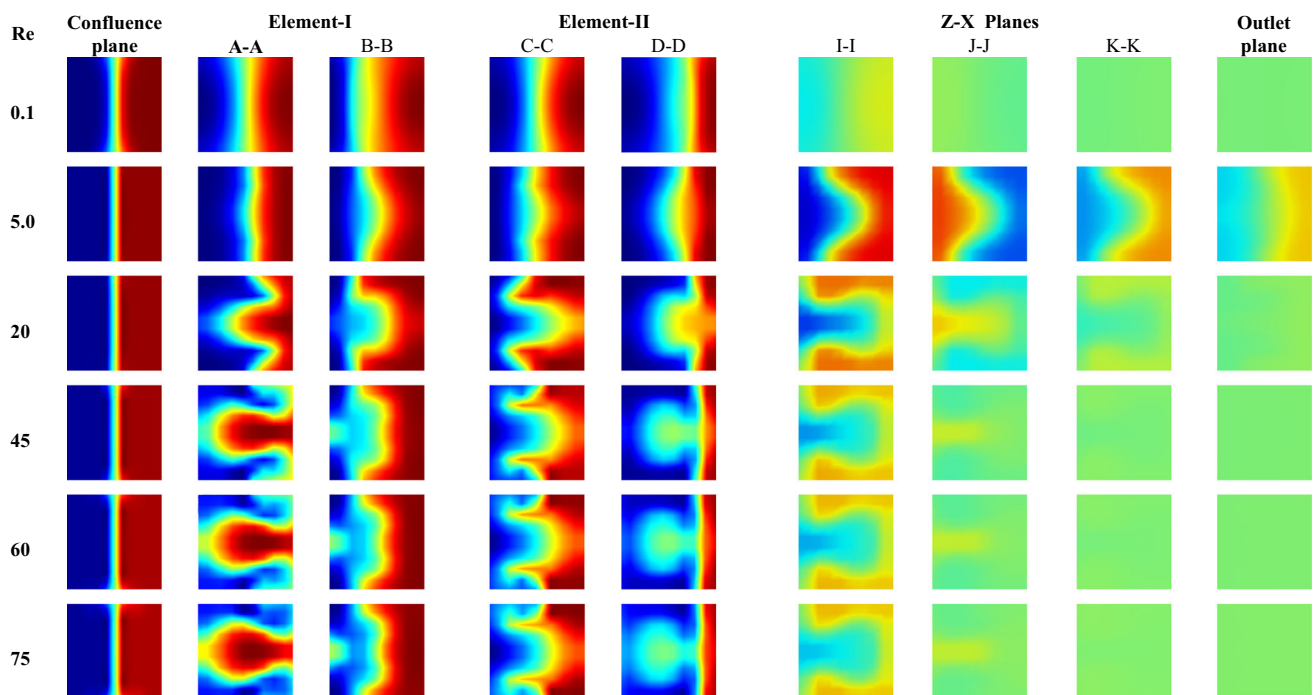
Fig. 8 Predicted concentration distributions at different planes for micromixer with ESAR elements with unbalanced split for Re = 0.1, 5, 20, 45, 60, and 75
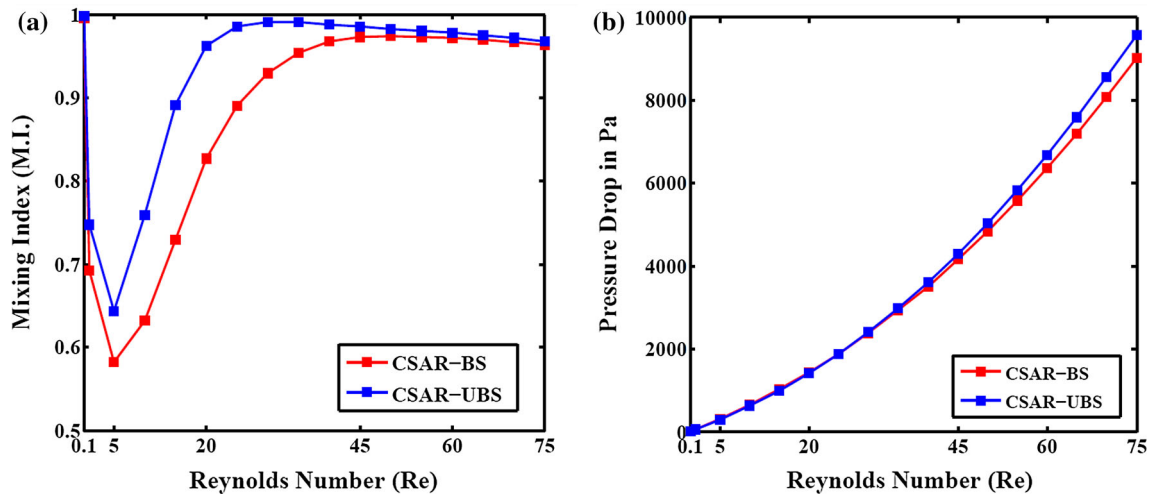
4.3 Overall performance analysis

The performance characteristics based comparison of micromixers with CSAR and ESAR elements is carried out and results are shown in Figs. 9, 10 and 11, respectively.
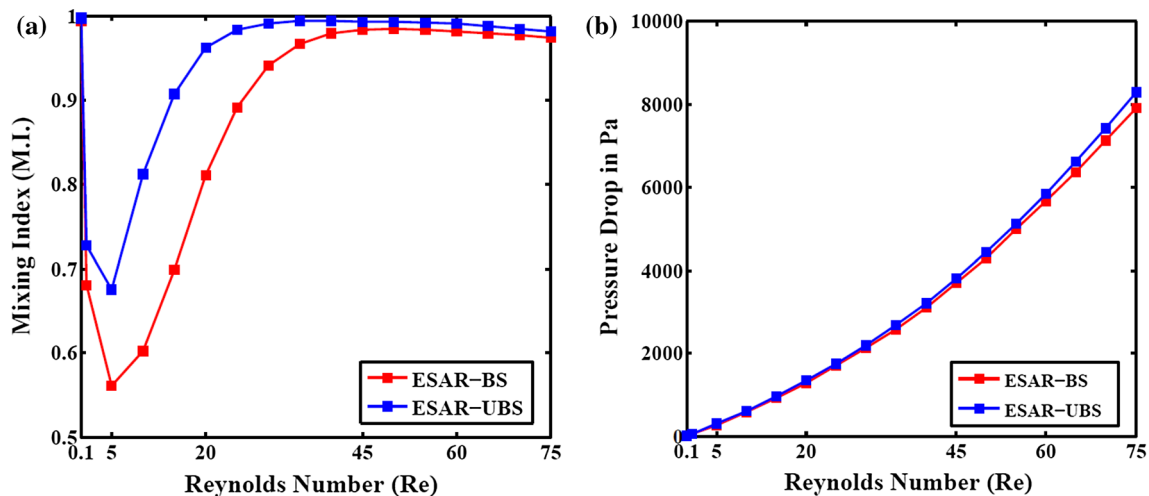
4.3.1 Mixing index

The mixing index is calculated at the outlet plane i.e. y–z plane at 10.5 mm distance in axial direction. The mixing performance of the micromixers with CSAR elements with balanced and unbalanced split has been evaluated for different Reynolds numbers by numerical simulation. Figures 9a and 10a shows the results of numerical simulation for the mixing performance as a function of balanced and

unbalanced split for Reynolds numbers ranging from 0.1 to 75. The unbalanced collision is effective in mixing the fluids for all the Reynolds numbers that are investigated in the present study.

The mixing index has been evaluated on cross-sectional planes located at different location in axial direction as depicted in Table 4. In addition to this, results of the mixing index as a function of axial distance are shown in Figs. 11, 12, and 13 for microcmixers with CSAR and ESAR elements with balanced and unbalanced split. Here, the mixing indices are calculated cross-sectional planes A–A, B–B, C–C, D–D, E–E, F–F, G–G, H–H and outlet plane in axial direction. The micromixers show nearly identical and relatively high rate of mixing along the channel length for both micromixers with unbalanced split as shown in

Fig. 9 Evaluation of overall performance **a** mixing index at the exit cross-section, **b** pressure drop of the micromixers having CSAR elements with balanced split as well as unbalanced split versus the Reynolds number
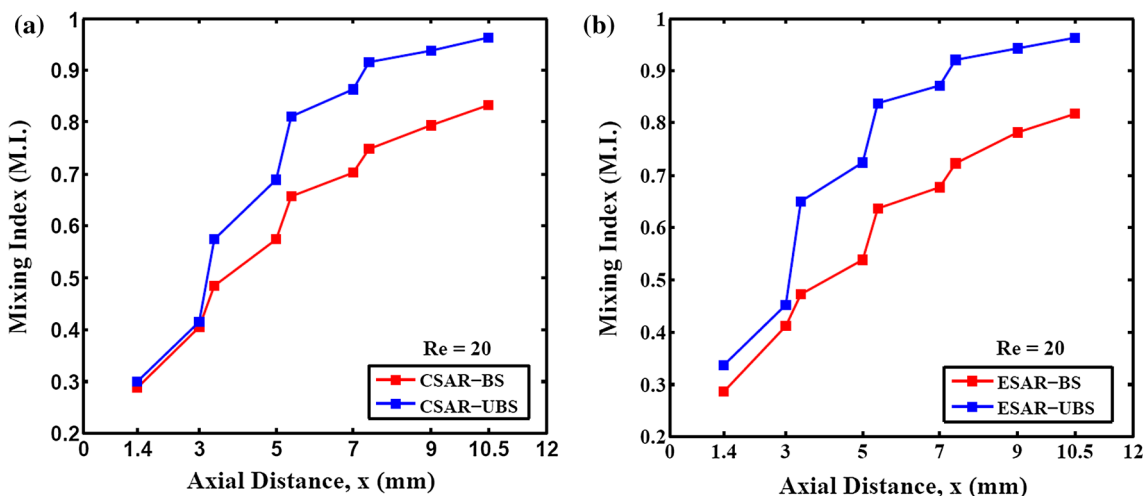

Fig. 10 Evaluation of overall performance **a** mixing index at the exit cross-section, **b** pressure drop of the micromixers having ESAR elements with balanced split as well as unbalanced split versus the Reynolds number
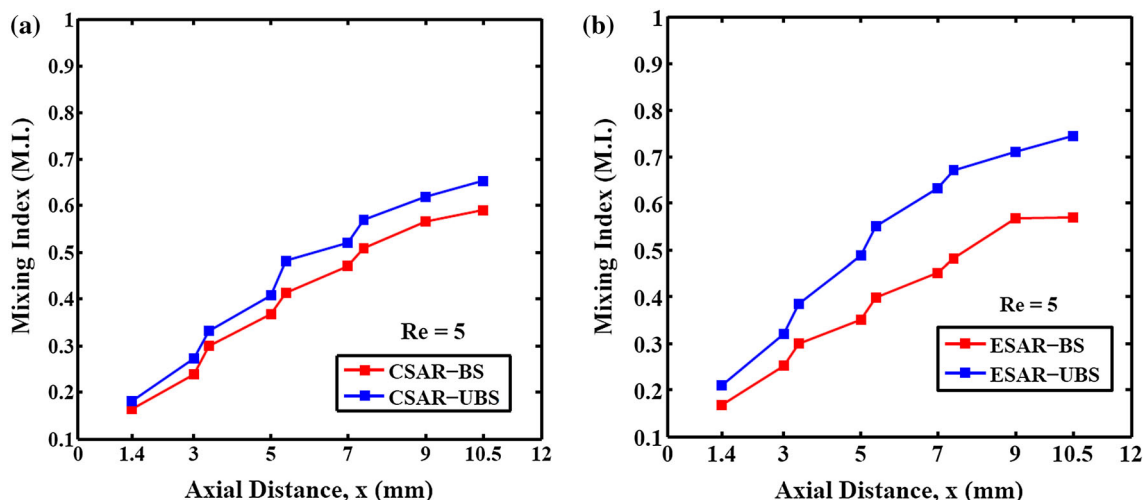
Fig. 11 Variation of mixing index along the mixing channel for **a** micromixer with CSAR elements, **b** micromixer with ESAR elements, respectively at Re = 5
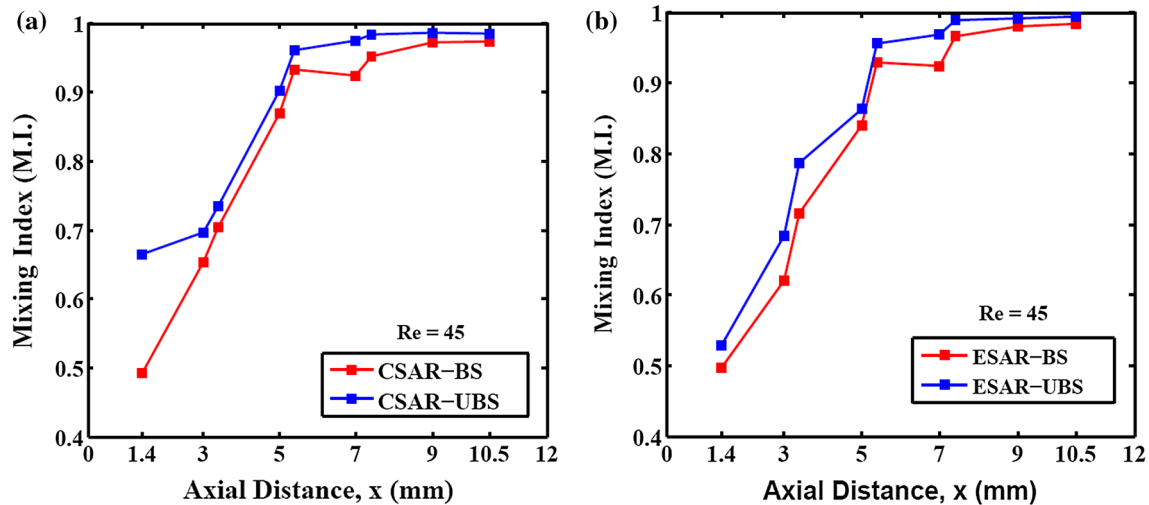

Fig. 12 Variation of mixing index along the mixing channel for **a** micromixer with CSAR elements, **b** micromixer with ESAR elements, respectively at Re = 20

Fig. 11. The mixing index rapidly increases after the each SAR element as indicated in the Figs. 11, 12, and 13 for Re = 5, Re = 20 and Re = 45, respectively. This enhanced mixing index is due to the SAR mechanism and collision between the streams of fluids. The result of mixing index along the axial direction gives an idea about the length of the micromixer required to attain complete mixing of the fluid for particular application. This is due to the difference between the inertias in the major and minor sub-channels of CSAR and ESAR elements. The mixing in the present micromixer is due to the combined effect of unbalanced collisions of the fluid streams, chaotic advection and SAR mechanism. The mixing is promoted by the vortices generated by the centrifugal forces on the fluid.

4.3.2 Pressure drop

The high pressure drop is directly related to the great energy dissipation that is unexpected in the actual mixing process. Therefore, the pressure drop for micromixers with CSAR and ESAR with balanced and unbalanced split as a function of the Reynolds number is illustrated in Figs. 9b and 10b, respectively, wherein the pressure drop increase with an increase in the Reynolds number. The pressure drops are small for at lower Reynolds numbers for both micromixers CSAR and ESAR. The increase pressure gradient becomes larger at Re > 20, wherein the more intense chaotic advection takes place. The diverse behavior on flow field occurs immediately beyond Re = 20, and is enhanced steadily as the Reynolds number increased. Consequently mixing quality is enhanced. The pressure

Fig. 13 Variation of mixing index along the mixing channel for **a** micromixer with CSAR elements, **b** micromixer with ESAR elements, respectively at Re = 45

drop is maximum for micromixers with unbalanced splits of both types SAR elements. However, micromixer with ESAR elements has the least pressure drop as compared to micromixer with CSAR elements in the Re range of 0.1–75 studied here. This is due to the more length of curvature for the CSAR elements as compared to ESAR elements.

5 Conclusion

In the present work, the detailed flow field analysis and mixing characteristics of two micromixers viz. wavy micromixer with CSAR and ESAR elements have been numerically investigated by using two representative types of splits i.e. balanced and unbalanced splits. A wide range of the Reynolds number (Re = 0.1–75) has been employed. At low Reynolds numbers, the mixing in micromixers with CSAR and ESAR elements is mainly dominated by diffusion as a result of more residence time. Hence the increased Re (i.e. Re = 1 and Re = 5) shortens the residence time, leading to the decreased mixing index. The mixing is diffusion dominated up to Re = 5. Beyond Reynolds number of 5, the mixing is enhanced by the gradual intensive chaotic advection. Therefore, the mixing indices of all micromixers with CSAR and ESAR increase as the Reynolds number increased. The micromixers with CSAR and ESAR with unbalanced splits exhibit the comparable superiority in mixing performance beyond the Reynolds number of 5. Furthermore, in all the four micromixers, the pressure drop rapidly increase with the Reynolds number as a result of the gradual enhanced chaotic advection.

In the flow downstream for the micromixers, the two fluids contacted each other along the height of the channel or at the interface between two fluids and suffered the effects of separation, split and recombination and chaotic advection. Hence, the mixing region is increased. Thus performance of proposed micromixers with SAR elements is enhanced due to larger the mixing region which in turn helps in better mixing of the fluids. Also, for mixing enhancement three approaches are utilized to improve mixing: the centrifugal forces due to wavy microchannel cause fluids to produce secondary flows, SAR action due to CSAR and ESAR elements; the impingement effect. Furthermore, the two fluids are folded into each other due to the secondary flow combined with the SAR effect and the impingement effect. Notably, due to the increases of the interfaces of the two fluids, mixing is improved in case micromixer with ESAR elements with unbalanced splits. At low Re, $0.1 < Re < 5$, viscous forces in the fluid are larger than inertial forces, thus inertia can be neglected. Mixing within the stated range of the Re is dominated by pure molecular diffusion. The mixing index then decreases as the Re increases within the range of 0.1–5. The secondary flow is negligible at low Reynolds number and mixing is dominated only by molecular diffusion. The mixing index increases abruptly with increasing Re when Re is greater than 5; the increased inertial force enlarges the contact area between two fluids. At Re > 5, the interface between the two fluids is greatly affected by the secondary flow and SAR effect which in turn promote enhanced mixing of fluids.

The micromixer with ESAR elements having unbalanced split exhibited better mixing performance than the micromixer with CSAR elements having unbalanced split throughout the tested range of Reynolds numbers. The pressure drop in the micromixer with ESAR elements is less than that in the micromixer with CSAR elements. Therefore, the proposed micromixer with ESAR element

shows good mixing performance in the Reynolds number range of 20–75.

Comparing the proposed CSAR and ESAR element based micromixers with the wavy micromixers without SAR elements proposed by the open literatures, the significant enhancement in mixing index has been observed in our proposed design with relatively small increase in pressure drop. In addition to this the proposed micromixers have significantly higher mixing sensitivity due to SAR elements. Thus proposed micromixer design is more promising to apply in LOC.

References

Alam A, Kim KY (2012) Analysis of mixing in a curved microchannel with rectangular grooves. Chem Eng J 181:708–716

Ansari MA, Kim KY, Anwar K, Kim SM (2010) A novel passive micromixer based on unbalanced splits and collisions of fluid streams. J Micromech Microeng 20(5):055007

Cheri MS, Latifi H, Moghaddam MS, Shahraki H (2013) Simulation and experimental investigation of planar micromixers with short-mixing-length. Chem Eng J 234:247–255

Cortes-Quiroz CA, Azarbadegan A, Zangeneh M (2014) Evaluation of flow characteristics that give higher mixing performance in the 3-D T-mixer versus the typical T-mixer. Sens Actuators B 202:1209–1219

Das SS, Patowari PK (2018) Fabrication of serpentine micro-channels on glass by ultrasonic machining using developed micro-tool by wire-cut electric discharge machining. Int J Adv Manuf Technol 95(5–8):3013–3028

Das SS, Tilekar SD, Wangikar SS, Patowari PK (2017) Numerical and experimental study of passive fluids mixing in micro-channels of different configurations. Microsyst Technol 23(12):5977–5988

Gidde RR, Pawar PM, Ronge BP, Misal ND, Kapurkar RB, Parkhe AK (2017) Evaluation of the mixing performance in a planar passive micromixer with circular and square mixing chambers. Microsyst Technol 24(6):2599–2610

Gidde RR, Shinde AB, Pawar PM, Ronge BP (2018) Design optimization of a rectangular wave micromixer (RWM) using Taguchi based grey relational analysis (GRA). Microsyst Technol 1–16

Hardt S, Drese KS, Hessel V, Schonfeld F (2005) Passive micromixers for applications in the microreactor and μTAS fields. Microfluid Nanofluid 1(2):108–118

Izadpanah E, Hekmat MH, Azimi H, Hoseini H, Rabiee MB (2018) Numerical simulation of mixing process in T-shaped and DT-shaped micromixers. Chem Eng Commun 205(3):363–371

Li J, Xia G, Li Y (2013) Numerical and experimental analyses of planar asymmetric split-and-recombine micromixer with dislocation sub-channels. J Chem Technol Biotechnol 88(9):1757–1765

Lin Y (2015) Numerical characterization of simple three-dimensional chaotic micromixers. Chem Eng J 277:303–311

Liu RH, Stremler MA, Sharp KV, Olsen MG, Santiago JG, Adrian RJ, Aref H, Beebe DJ (2000) Passive mixing in a three-dimensional serpentine microchannel. J Microelectromech Syst 9(2):190–197

Mouza AA, Patsa CM, Schonfeld F (2008) Mixing performance of a chaotic micro-mixer. Chem Eng Res Des 86(10):1128–1134

Nguyen NT, Wu ZG (2004) Micromixers—a review. J Micromech Micro Eng 15(2):R1–R16

Sheu TS, Chen SJ, Chen JJ (2012) Mixing of a split and recombine micromixer with tapered curved microchannels. Chem Eng Sci 71:321–332

Shih TR, Chung CK (2008) A high-efficiency planar micromixer with convection and diffusion mixing over a wide Reynolds number range. Microfluid Nanofluid 5(2):175–183

Stroock AD, Dertinger SK, Ajdari A, Mezic I, Stone HA, Whitesides GM (2002) Chaotic mixer for microchannels. Science 295(5555):647–651

The HL, Ta BQ, Le TH, Dong T, Thoi TN, Karlsen F (2015) Geometric effects on mixing performance in a novel passive micromixer with trapezoidal-zigzag channels. J Micromech Microeng 25(9):094004

Tran-Minh N, Dong T, Karlsen F (2014) An efficient passive planar micromixer with ellipse-like micropillars for continuous mixing of human blood. Comput Method Program Biomed 117(1):20–29

Wangikar SS, Patowari PK, Misra RD (2017) Numerical and experimental investigations on the performance of a serpentine microchannel with semicircular obstacles. Microsyst Technol 24(8):3307–3320

Wong SH, Bryant P, Ward M, Wharton C (2003) Investigation of mixing in a cross shaped micromixer with static mixing elements for reaction kinetics studies. Sens Actuators B 95(1–3):414–424

Xia G, Li J, Tian X, Zhou M (2012) Analysis of flow and mixing characteristics of planar asymmetric split-and-recombine (P-SAR) micromixers with fan-shaped cavities. Ind Eng Chem Res 51(22):7816–7827

Xia GD, Li YF, Wang J, Zhai YL (2016) Numerical and experimental analyses of planar micromixer with gaps and baffles based on field synergy principle. Int Commun Heat Mass Transf 71:188–196